Available online at www.sciencedirect.com
ScienceDirect
Metabolism Clinical and Experimental 60 (2011) 513 – 522
Metabolism
Clinical and Experimental
www.metabolismjournal.com

Fenofibrate suppresses microvascular inflammation and apoptosis through adenosine monophosphate–activated protein kinase activation

Atsuko Tomizawa[a], Yoshiyuki Hattori[a,*], Teruo Inoue[b], Sachiko Hattori[a], Kikuo Kasai[a]

[a]*Department of Endocrinology and Metabolism, Dokkyo University School of Medicine, Mibu, Tochigi 321-0293, Japan*
[b]*Department of Cardiovascular Medicine, Dokkyo University School of Medicine, Mibu, Tochigi 321-0293, Japan*

Received 4 January 2010; accepted 19 April 2010

Abstract

The Fenofibrate Intervention and Event Lowering in Diabetes study demonstrated that treatment with fenofibrate in individuals with type 2 diabetes mellitus not only reduced nonfatal coronary events but also diminished the need for laser treatment of diabetic retinopathy and delayed the progression of diabetic nephropathy. However, the mechanism by which fenofibrate may have altered the microvasculature remains unclear. We thus investigated the effect of fenofibrate on human glomerular microvascular endothelial cells (HGMEC). Treatment of HGMEC with fenofibrate resulted in transient activation of adenosine monophosphate–activated protein kinase (AMPK), thereby inducing the phosphorylation of Akt and endothelial nitric oxide synthase, leading to nitric oxide production. We compared AMPK activation induced by bezafibrate and WY14643 with that induced by fenofibrate in HGMEC as well as HepG2 cells. Only fenofibrate activated AMPK in HGMEC. Fenofibrate also inhibited nuclear factor–κB activation by advanced glycation end-products, thereby suppressing the expression of various adhesion molecule genes in HGMEC. Suppression of fenofibrate-induced inhibition of nuclear factor–κB activation was observed in cells treated with AMPK small interfering RNA or compound C. Furthermore, fenofibrate was observed to significantly suppress apoptosis of HGMEC in hyperglycemic culture medium. Treatment with compound C or Nw-nitro-L-arginine methyl ester (L-NAME) abolished the suppressive effect of fenofibrate on HGMEC apoptosis. Our findings suggest that fenofibrate might exert a protective effect on the microvasculature by suppressing inflammation and apoptosis through AMPK activation beyond its lipid-lowering actions.

1. Introduction

The Fenofibrate Intervention and Event Lowering in Diabetes (FIELD) study recruited a low-risk population with a lipid profile that would be more usually treated with a statin [1]. The FIELD study showed a nonsignificant 11% reduction (P = .16) in the primary end point of coronary events and a significant 11% benefit on the secondary end point of cardiovascular events and procedures (P = .04). Most of the benefits were seen in primary prevention and nonfatal myocardial events. In addition, fenofibrate unexpectedly showed possible benefits on microvascular disease end points, including microalbuminuria and retinopathy [2,3]. Furthermore, it has very recently reported that treatment of fenofibrate was associated with a lower risk of amputations, particularly minor amputations without known large vessel diseases in FIELD study [4]. These microvascular benefits of fenofibrate are appealing, but its mechanism is unknown.

Ido et al [5] and Cacicedo et al [6] first demonstrated that adenosine monophosphate–activated protein kinase (AMPK) activation protects macrovascular endothelium against apoptosis and other abnormalities caused by glucose, fatty acids, and tumor necrosis factor (TNF) α. Recently, fenofibrate was found to activate AMPK in vascular endothelial cells [7]. Adenosine monophosphate–activated protein kinase has been shown to mediate the beneficial and bioprotective effects of several drugs and adipocytokines, such as metformin, thiazolidine derivatives, adiponectin, and leptin [8-11]. Thus, we hypothesized that the microvascular

* Corresponding author. Tel.: +81 282 87 2150; fax: +81 282 86 4632.
E-mail address: yhattori@dokkyomed.ac.jp (Y. Hattori).

0026-0495/$ – see front matter © 2011 Elsevier Inc. All rights reserved.
doi:10.1016/j.metabol.2010.04.020

benefits of fenofibrate might be caused through AMPK activation in microvascular endothelial cells.

In the present study, we confirmed that fenofibrate activates AMPK in microvascular endothelial cells and examined whether the AMPK activation is mediated via peroxisome proliferator-activated receptor (PPAR) α activation. The capability of fenofibrate to activate AMPK was compared with bezafibrate in endothelial cells and hepatic cells. We then investigated the effects of fenofibrate on the endothelial inflammation and apoptosis under diabetic condition, and whether possible effects are mediated through AMPK activation.

2. Materials and methods

2.1. Cell culture

Human glomerular microvascular endothelial cells (HGMEC) were obtained from Sanyo Chemical Industries (Tokyo, Japan) and cultured in CSC complete defined medium (Cell System, Kirkland, WA). The cells in this experiment were used within 3 to 4 passages and were examined to ensure that they demonstrated the specific characteristics of endothelial cells. Mouse SVEC4 cells (axillary lymph node, vascular endothelial: ATCC, CRL-2181) were also cultured in Dulbecco modified Eagle medium (Nichirei Biosciences, Tokyo, Japan) containing 10% fetal calf serum and observed to demonstrate the typical cobblestone morphologic appearance of endothelial cells. HepG2 cells, a human hepatoma cell line (ATCC, HB-8065), were cultured in Dulbecco modified Eagle medium containing 10% fetal calf serum and used as hepatocytes.

2.2. Western blot analysis

Human glomerular microvascular endothelial cells were lysed in buffer comprising 10 mmol/L Tris, pH 7.4, 100 mmol/L NaCl, 1 mmol/L EDTA, 1 mmol/L EGTA, 1 mmol/L NaF, 20 mmol/L $Na_4P_2O_7$, 2 mmol/L Na_3VO_4, 0.1% sodium dodecyl sulfate (SDS), 0.5% sodium deoxycholate, 1% Triton X-100 (Sigma Chemical Co, St. Louis, MO), 10% glycerol, 10 μg/mL leupeptin, 60 μg/mL aprotinin, and 1 mmol/L phenylmethanesulfonyl fluoride. Human glomerular microvascular endothelial cell lysates were resolved on SDS–polyacrylamide gel electrophoresis (PAGE) according to standard protocols. After being transferred to membranes, the samples were immunoblotted with primary antibodies, followed by secondary antibodies conjugated with horseradish peroxidase. Bands were revealed by use of an enzyme-linked chemiluminescence detection kit (Amersham Biosciences, Piscataway, NJ), and density was quantified with LumiVision Analyzer (Aisin, Kariya, Japan). Primary antibodies used were as follows: antiphosphorylated AMPKα (Thr-172), anti-AMPKα, antiphosphorylated acetyl–coenzyme A carboxylase (ACC) (Ser-79), anti-ACC, antiphosphorylated endothelial nitric oxide synthase (eNOS) (Ser-1177), antiphosphorylated Akt (Thr-308), anti-Akt, antiphosphorylated IκBα, anti-IκBα (Cell Signaling Technology, Beverly, MA), and anti-eNOS monoclonal antibody (BD Biosciences, San Jose, CA).

2.3. NOx measurement

Nitric oxide production within monolayers of endothelium was measured as previously reported [12]. After 1 hour of incubation, nitrite and nitrate (NOx) levels ($NO2^-$ and $NO3^-$) in the medium were measured with an automated NO detector/high-performance liquid chromatography system (ENO10; Eicom, Kyoto, Japan).

2.4. Determination of eNOS activity

Citrulline synthesis was measured by modification of a previously described technique [13,14]. Cell monolayers were incubated at 37°C for 30 minutes in Hanks balanced salt solution (pH 7.4) containing 0.5% fetal bovine serum. Subsequently, cells were incubated with fenofibrate in the presence of 10 μmol/L L-arginine and 3.3 μCi/mL L-[^{3}H] arginine. After 30 minutes, the reaction was stopped with cold phosphate-buffered saline containing 5 mmol/L L-arginine and 4 mmol/L EDTA, after which the cells were denaturated with 96% ethanol. After evaporation, the soluble cellular components were dissolved in 50 mmol/L HEPES and 5 mmol/L EDTA (pH 5.5), and applied to 2-mL columns of Dowex AG50WX-8 (Na^+ form; Muromachi Kagaku Kogyo Kaisha, Ltd, Tokyo, Japan). Radioactivity corresponding to [^{3}H]citrulline within the eluate was quantified by liquid scintillation counting. This was expressed as femtomoles per milligram of cell protein. Basal [^{3}H]citrulline synthesis was determined from Nw-nitro-L-arginine methyl ester (L-NAME) (1 mmol/L, 30-minute preincubation)–inhibitable radioactivity in unstimulated cells, which was not always detectable.

2.5. Nuclear factor–κB activation

To study nuclear factor (NF)–κB activation, SVEC4 cells were stably transfected with a *cis*-reporter plasmid containing the luciferase reporter gene linked to 5 repeats of NF-κB binding sites (pNFκB-Luc; Stratagene, La Jolla, CA), as previously described [15]. For this, the pNFκB-Luc plasmid was transfected together with a pSV2neo helper plasmid (Clontech, Palo Alto, CA) into SVEC4 cells using a FuGEN 6 transfection reagent (Boehringer Mannheim, Mannheim, Germany). The cells were then cultured in the presence of G418 (Clontech) at a concentration of 500 μg/mL, and the medium was replaced every 2 to 3 days. Approximately 3 weeks after transfection, G418-resistant clones were isolated using a cloning cylinder and analyzed individually for expression of luciferase activity. Several clones were also selected for analysis of NF-κB activation. Luciferase activity was measured using a luciferase assay kit (Stratagene).

We also measured changes in the levels of NF-κB p50 and p65 in nuclear extracts from HGMEC using a

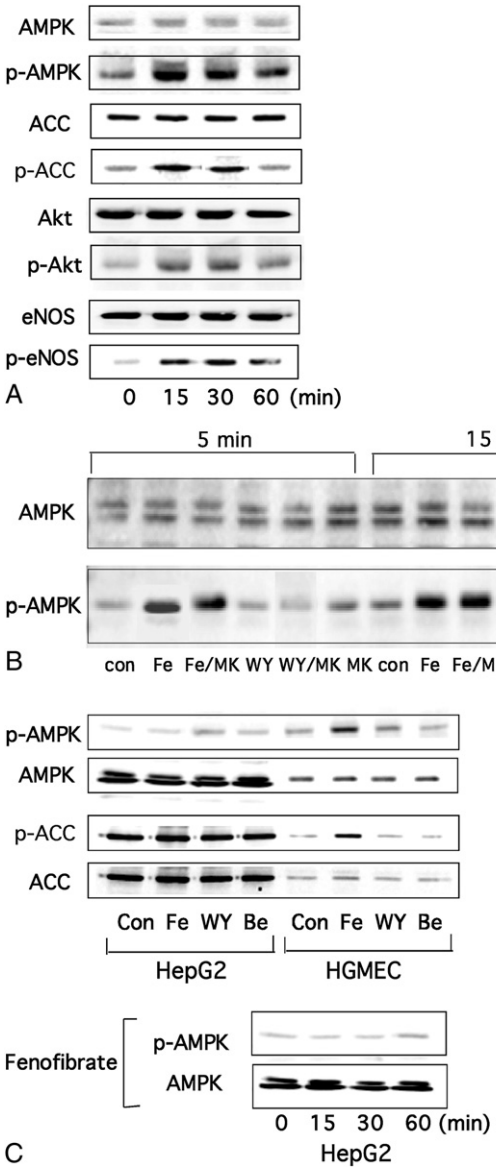

Fig. 1. A, Fenofibrate activates AMPK in microvascular endothelial cells. Human glomerular microvascular endothelial cells were treated with 100 μmol/L fenofibrate for the indicated periods before lysis, after which cell lysates were probed with antibodies specific for AMPK, ACC, Akt, or eNOS, or their phosphorylated forms. B, Peroxisome proliferator–activated receptor α antagonist MK886 did not affect fenofibrate-induced AMPK activation, and PPARα agonist WY14643 scarcely activated AMPK in HGMEC. C, Fenofibrate activates AMPK in microvascular endothelial cells but not in hepatic cells. HepG2 cells and HGMEC were treated with fenofibrate, WY14643, or bezafibrate for 15 minutes and analyzed with antibodies specific for AMPK or ACC. Lower figure in Fig. 1C shows that fenofibrate did not activate AMPK during indicated period in HepG2. Fe indicates fenofibrate (100 μmol/L); MK, MK886 (100 μmol/L); WY, WY14643 (100 μmol/L); Be, bezafibrate (100 μmol/L).

transcription factor assay kit (Active Motif Japan, Tokyo, Japan). Nuclear extracts were prepared with an NE-PER nuclear extraction reagent (Pierce, Rockford, IL), after which p50 and p65 were quantified using Jurkat nuclear extract as the standard.

2.6. IκB kinase assay

IκB kinase (IKK) activity was examined using an immune complex kinase assay with GST-IκBα (1-55) as the substrate, as previously described [16]. Briefly, the cells were solubilized in ice-cold buffer and then centrifuged at 15 000*g* for 20 minutes. IκB kinase α and IKKβ were recovered from the cell lysate by immunoprecipitation, after which the immune complexes were incubated with 20-μL reaction buffer containing 20 mmol/L HEPES/NaOH (pH 7.4), 10 mmol/L $MgCl_2$, 50 mmol/L NaCl, 100 mmol/L Na_3VO_4, 20 mmol/L β-glycerophosphate, 1 mmol/L dithiothreitol (DTT), 100 μmol/L adenosine triphosphate, 0.1 μCi [γ-^{32}P]adenosine triphosphate, and 10 μg GST-IκBα (1-55) at 30°C for 20 minutes. After SDS-PAGE, the phosphorylation of GST-IκBα was estimated using an imaging plate (Fuji Film, Tokyo, Japan).

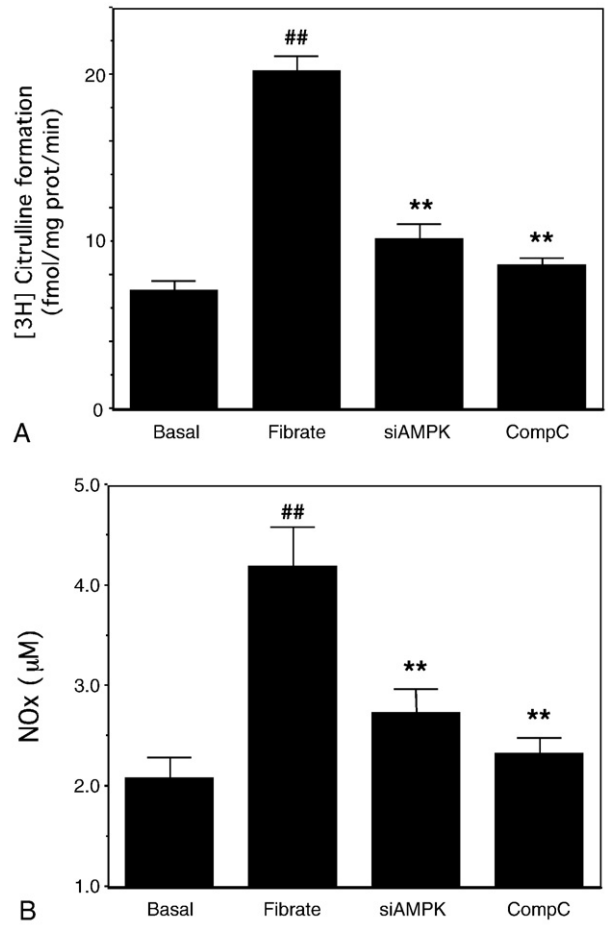

Fig. 2. Fenofibrate increased eNOS activity (A) and NO production (B) in HGMEC, which are significantly attenuated in cells transfected with AMPK siRNA (10 nmol/L) or treated with an AMPK inhibitor compound C (1 mmol/L). Results represent the mean ± SEM (n = 4). $^{\#\#}P < 01$ vs basal; $^{**}P < .01$ vs fenofibrate (only).

2.7. Preparation of AGE protein

Advanced glycated end-product (AGE)–bovine serum albumin (BSA) was prepared as described previously [17]. Bovine serum albumin (fraction V) was incubated under sterile conditions with D-glyceraldehyde for 7 days. Unincorporated sugars were then removed by dialysis against phosphate-buffered saline. Control nonglycated BSA was incubated in the same conditions with the exception of the absence of reducing sugars. Preparations were tested for endotoxin using Endospecy ES-20S system (Seikagaku, Tokyo, Japan) where no endotoxin was detectable. The extent of lysine modification (percentage) of modified BSA preparations was approximately 65% for glycer-AGE-BSA.

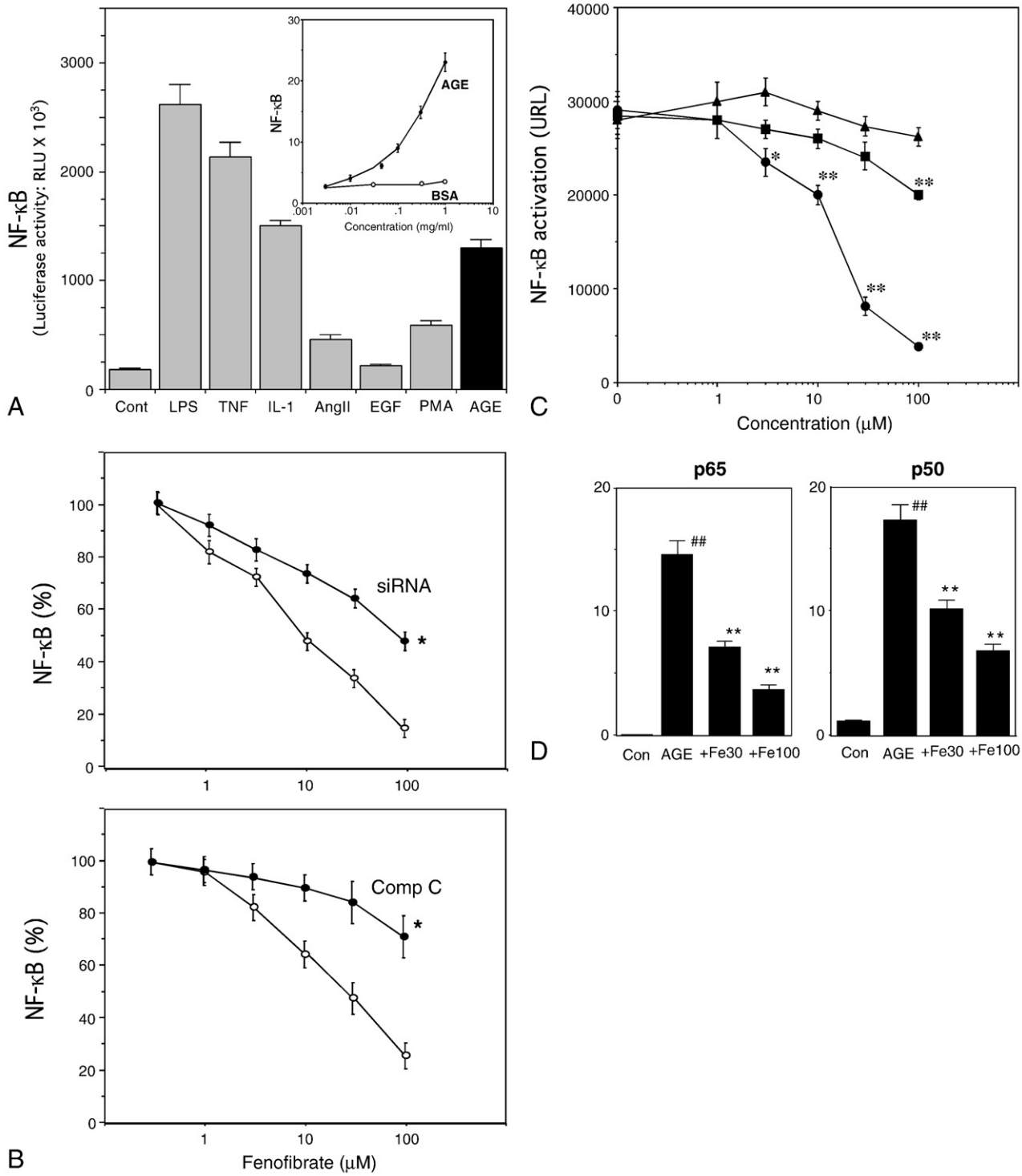

2.8. Small interfering RNA transfection

The day before transfection, plates were inoculated with an appropriate number of HGMEC or SVEC4 cells in serum-containing medium to ensure approximately 70% confluence the following day. AMPKα1 small interfering RNA (siRNA) (Santa Cruz Biotechnology, Santa Cruz, CA) mixed with siLentFect (Bio-Rad, Tokyo, Japan) was added to the cells at a concentration of 10 nmol/L. Forty-eight hours after transfection, eNOS activity and NO production in HGMEC or AGE-BSA–induced NF-κB activity in SVEC4 cells was compared with those of control cells, respectively.

2.9. Real-time polymerase chain reaction of HGMEC messenger RNA

For quantitative measurement of messenger RNA (mRNA), 2 μg of total RNA was treated with DNase I (Sigma-Aldrich Chemical, St Louis, MO) for 15 minutes and subsequently used for complementary DNA synthesis. Reverse transcription was performed using a SuperScript preamplification system (Gibco BRL, Gaithersburg, MD) with random oligonucleotide primers. The following primers were used: intracellular adhesion molecule-1 (ICAM-1) forward 5′-CCGGAAGGTG-TATGAACTGA-3′, reverse 5′-GGCAGCGTAGGG-TAAGGTT-3’; vascular cell adhesion molecule-1 (VCAM-1) forward 5′-GGCAGAGTACGCAAACACTT-3′, reverse 5′-GGCTGTAGCTCCCCGTTAG-3′; E-selectin forward 5′-GCCTTGAATCAGACGGAAGC-3′, reverse 5′-TGATGGGTGTTGCGGTTTC-3′; GAPDH forward 5′-GGAGAAGGCTGGGGCTCAT-3′, reverse 5′-TGATGG-CATGGACTGTGGTC-3′. A typical reaction (50 μL) contained 1/50 of reverse transcription–generated complementary DNA and 200 nmol/L of primer in 1× SYBR Green RealTime Master Mix (Toyobo, Tokyo, Japan) buffer. The polymerase chain reactions were carried out in a LineGene system (BioFlux, Tokyo, Japan) under the following conditions: 95°C for 5 minutes and 40 cycles at 95°C for 15 seconds, 60°C for 15 seconds, and 72°C for 30 seconds.

2.10. Apoptosis measurement

Human glomerular microvascular endothelial cells were incubated with 24.5 mmol/L glucose (final concentration, 30 mmol/L) or with 24.5 mmol/L mannitol (widely used osmotic control) for 6 days (long-term exposure to mimic chronic hyperglycemia). After this, cell viability was assessed using the MTT colorimetric assay [18]. MTT, when taken up by living cells, is converted from a yellow to a water-insoluble blue precipitate by cellular dehydrogenases. Apoptosis was evaluated using Guava EasyCyte Mini Flow cytometry system (Millipore). The ViaCount Assay distinguishes viable and nonviable cells based on differential permeabilities of 2 DNA-binding dyes in the Guava ViaCount Reagent. The nuclear dye stains only nucleated cells, whereas the viability dye brightly stains dying cells to distinguish viable, apoptotic, and dead cells. The Guava Nexin Annexin V Assay was also used to assess early apoptosis, which relies on the translocation of phosphatidyl serine to the outer surface of the cell membrane [19,20].

2.11. Statistical analysis

Data are presented as the mean ± SEM. Multiple comparisons were evaluated by analysis of variance followed by Fisher protected least significant difference test. A value of $P < .05$ was considered statistically significant.

3. Results

3.1. Fenofibrate activates AMPK in microvascular endothelial cells

Treatment of HGMEC with fenofibrate resulted in time-dependent activation of AMPK, as monitored by phosphorylation of AMPK and its down-stream target, ACC, (Fig. 1A), consistent with previously reported activation of AMPK in vascular endothelial cells by fenofibrate [7]. This may lead to eNOS phosphorylation and activation. Indeed, Ser-1177 phosphorylation of eNOS was observed at the peak of 30 minutes; and eNOS remained Ser-1177 phosphorylated at 60 minutes. Akt (protein kinase B) phosphorylation was observed with similar kinetics.

Fig. 1B shows the effect of PPARα inhibitor MK886 on fenofibrate- or PPARα activator WY14643-induced activation of AMPK. MK886 showed no effect on AMPK activation by fenofibrate, whereas WY14643 weakly induced AMPK activation at 15 minutes, which was barely influenced by MK886.

We compared AMPK activation induced by bezafibrate (another fibrate drug) and WY14643 with that induced by

Fig. 3. A, The effects of AGE-BSA and control agents on NF-κB–dependent transcriptional activity. SVEC4 cells (transfected with pNFκB-Luc) were left untreated (Cont) or were treated with LPS (10 μg/mL), TNFα (10 ng/mL), IL-1β (10 ng/mL), Ang II (100 nmol/L), EGF (100 ng/mL), PMA (100 nmol/L), or AGE-BSA (1 mg/mL). After 2 hours, cells were lysed; and luciferase activities were measured. Inset: The cells were treated with different concentrations of AGE-BSA (0.003-1 mg/mL) for 2 hours, after which luciferase activities were measured. Closed circles with AGE-BSA vs open circles with control BSA. B, Effects of AMPK siRNA transfection or AMPK inhibitor compound C treatment on fenofibrate-induced inhibition of AGE-BSA–induced NF-κB activation in SVEC4 cells. siRNA (10 nmol/L) or compound C (1 mmol/L) blunted fenofibrate-induced inhibition of NF-κB activity (closed circles). C, Fenofibrate, but not bezafibrate, dose-dependently suppressed AGE-BSA-induced NF-κB activation in SVEC4 cells. Cells were treated with various concentrations of fenofibrate (closed circles), bezafibrate (closed triangles), or WY14643 (closed squares), and then stimulated with AGE-BSA for 2 hours, after which luciferase activities were measured. Results represent the mean ± SEM (n = 4). $^{*}P < .05$; $^{**}P < .01$. D, Human glomerular microvascular endothelial cells were stimulated with AGE-BSA in the presence or absence of fenofibrate (Fe30: 30 μmol/L, Fe100: 100 μmol/L) for 30 minutes. Nuclear factor–κB p65 or p50 subunits were quantified within nuclear extracts using a transcription factor assay kit using Jurkat nuclear extract as the standard. Results represent the mean ± SEM (n = 4). $^{\#\#}P < .01$ vs Con; $^{**}P < .01$ vs AGE (only).

fenofibrate in HGMEC as well as HepG2 cells (from a hepatoma cell line). Only fenofibrate activated AMPK in HGMEC, whereas bezafibrate did not activate AMPK at all and WY14643 caused only minimal AMPK activation. Neither fenofibrate nor bezafibrate activated AMPK in Hep G2 cells, whereas WY14643 caused a modest increased in AMPK phosphorylation (Fig. 1C).

3.2. eNOS activity and NO production by fenofibrate in microvascular endothelial cells

To measure eNOS activity, HGMEC were incubated with fenofibrate for 30 minutes, after which citrulline synthesis was measured. The eNOS activity, measured in terms of citrulline production, was observed to increase with fenofibrate treatment. This increase in eNOS activity was significantly suppressed by treatment of HGMEC with an AMPKα1 siRNA or compound C (an AMPK inhibitor) (Fig. 2A).

Incubation of HGMEC with fenofibrate increased the concentration of bioactive NO in the supernatant of the cells (as measured by $NO2^-$ and $NO3^-$ levels). Examination of the time course showed a substantial increase in NO production for 1 hour, after which only a modest elevation in NO production was observed (data not shown). As shown in Fig. 2B, fenofibrate increased NO production, an increase significantly suppressed by treatment with AMPKα1 siRNA or compound C.

3.3. Fenofibrate inhibits NF-κB activation

We initially examined the AGE-BSA inducibility of NF-κB–mediated reporter gene expression in SVEC4 cells comparing with lipopolysaccharide (LPS), TNFα, interleukin (IL)-1β, amgiotensin II (Ang II), epidermal growth factor (EGF), and phorbol myristate acetate (PMA). LPS, TNFα, and IL-1β potently stimulated NF-κB–mediated reporter gene transcription in SVEC4 cells. Whereas Ang II and PMA weakly induced NF-κB–mediated reporter gene transcription, EGF had very little effect. AGE-BSA substantially activated NF-κB–mediated reporter gene transcription with potency comparable to that of IL-1β. Nuclear factor-κB–mediated reporter gene-dependent transactivation increased 7.5 fold relative to unstimulated levels in BSA-treated SVEC4 cells at 1 mg/mL (Fig. 3A).

We examined the effects of AMPKα1 siRNA or compound C on fenofibrate-induced inhibition of NF-κB activated by AGE-BSA. Induction of an NF-κB–mediated reporter gene expression by AGE-BSA was dose-dependently inhibited by fenofibrate, which was significantly attenuated in siRNA-transfected cells or compound C–treated cells (Fig. 3B).

The effect of bezafibrate and WY14643 on the AGE-BSA–induced NF-κB activation was compared with the inhibitory effect of fenofibrate on it. Fenofibrate dose-dependently diminished AGE-induced NF-κB activity, whereas bezafibrate did not affect the NF-κB activity at all concentrations used and WY14643 weekly inhibited the NF-κB activity at higher concentrations (Fig. 3C).

We also measured p50 and p65 in nuclear extracts from untreated HGMEC and those treated with AGE-BSA in the presence or absence of fenofibrate. Levels of p50 and p65 markedly increased 30 minutes after stimulation with AGE-BSA from very low levels. This increase was significantly attenuated by exposure to fenofibrate in a dose-dependent manner (Fig. 3D).

3.4. AGE-BSA stimulates IκB phosphorylation by inducing IKK activity, and fenofibrate inhibits AGE-BSA–induced IKK activity and IκB phosphorylation

We first determined whether AGE-BSA–induced NF-κB activation occurs through phosphorylation and subsequent

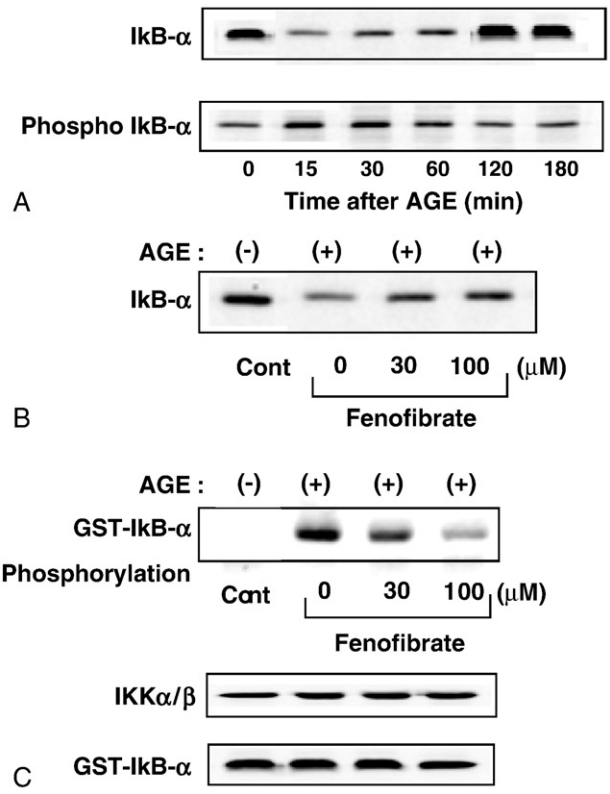

Fig. 4. A, Human glomerular microvascular endothelial cells were incubated with AGE-BSA for 0 to 180 minutes. The cells were lysed and subjected to Western blot analysis using anti-IκBα and anti–phospho-IκBα antibodies. B, The effect of fenofibrate on IκB-α degradation in human umbilical vein endothelial cells. Cells were incubated for 30 minutes with fenofibrate (30 and 100 μmol/L), followed by AGE-BSA for 15 minutes. Cells were then lysed and subjected to Western blot analysis using anti-IκBα antibody. C, The effect of fenofibrate on IKK activity in HGMEC. Cells were incubated for 30 minutes with fenofibrate (30 and 100 μmol/L), followed by AGE-BSA for 15 minutes. Cells were then lysed and immunoprecipitated with anti-IKKα/β antibody and used for kinase assay using recombinant IκB-α as a substrate. Note that equal band densities for IKKα/β- and IκB-α were observed. Similar results in 3 independent experiments were obtained, and representative photographs are shown.

degradation of IκB. To determine whether AGE-BSA causes IκBα phosphorylation in HGMEC, Western blot analysis using anti–phospho-Ser32 of IκBα antibody was performed. AGE-BSA induced IκB phosphorylation in 15 minutes, and decreased levels of phospho-IκBα were observed at 120 minutes. The blot was then reprobed with anti-IκB antibody, producing evidence of significant degradation within 15 to 30 minutes. After this, IκB synthesis was reactivated, possibly by NF-κB, by 120 minutes (Fig. 4A). Next, the effect of fenofibrate on AGE-BSA–induced IκBα degradation was determined 15 minutes after exposure to AGE-BSA. Fenofibrate partially inhibited AGE-BSA–induced IκBα degradation (Fig. 4B).

A radiolabeled, phosphorylated IκBα-specific band was detected in AGE-BSA–treated cells, whereas it was undetectable in untreated cells, demonstrating induction of IKK activity by AGE-BSA (Fig. 4C). IκB kinase activity was dose-dependently inhibited by treatment of the cells with fenofibrate (Fig. 4C). The remaining half of the immunoprecipitated samples were analyzed by Western blot analysis using anti-IKKα/β antibody, which showed identical expression levels of IKK. Identical amounts of IκB were also detected when an equal volume of kinase reaction mixture was loaded into the SDS-PAGE column, followed by Western blot analysis using anti-IκB antibody (Fig. 4C).

3.5. Fenofibrate inhibits induction of VCAM-1, E-selectin, and ICAM-1 mRNA

Incubation of HGMEC for 8 hours with AGE-BSA substantially induced the gene expression of VCAM-1, E-selectin, and ICAM-1. Induction of AGE-BSA–induced gene expression was markedly suppressed by cotreatment with a NF-κB inhibitor, BAY11-7082, which selectively and irreversibly inhibits cytokine-induced IκB phosphorylation, suggesting that the induction of these genes is NF-κB dependent (data not shown). Coincubation with 100 μmol/L fenofibrate markedly diminished AGE-BSA–induced gene expression of VCAM-1, E-selectin, and ICAM-1, in which effects of fenofibrate were abrogated by the presence of compound C (Fig. 5).

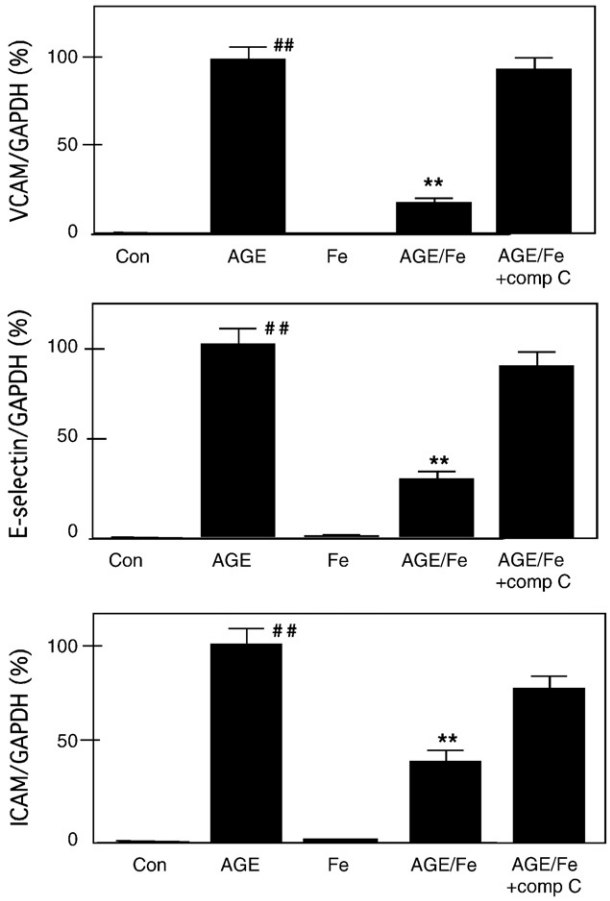

Fig. 5. Effects of fenofibrate on AGE-BSA–induced VCAM-1, E-selectin, and ICAM-1 mRNA expression in HGMEC. Fenofibrate (Fe: 100 μmol/L) significantly inhibited VCAM-1, E-selectin, and ICAM-1 mRNA levels, which were reversed by compound C (1 mmol/L). Messenger RNA levels are expressed as a ratio of GAPDH (:100% as VCAM-1/GAPDH, E-selectin/GAPDH, and ICAM-1/GAPDH stimulated with TNFα). Each bar represents the mean ± SEM (n = 4). $^{\#\#}P < 01$ vs Con; $^{**}P < .01$ vs AGE (only).

3.6. Fenofibrate attenuates cell apoptosis induced by high glucose condition

Human glomerular microvascular endothelial cells were exposed to 30 mmol/L glucose for 6 days to mimic chronic hyperglycemia. Because high glucose increases osmolarity, HGMEC were also exposed to 24.5 mmol/L mannitol (+5.5 mmol/L glucose in the culture medium), which is commonly used as an osmotic control. To analyze the effect of high glucose/osmolarity in cell viability, we used the MTT assay [16]. High glucose significantly decreased the MTT reduction to 73.8% ± 3.2% of the control, whereas mannitol did not cause a significant decrease in the MTT reduction (92.8% ± 11.5% of the control) (Fig. 6A).

To confirm whether the hyperglycemia-induced reduction in MTT reduction was due to endothelial cell death, we quantified endothelial cell apoptosis by the ViaCount assay in which the nuclear dye stains only nucleated cells, whereas the viability dye brightly stains dying cells to distinguish viable, apoptotic, and dead cells. High glucose significantly increased the number of apoptotic cells (10.8% ± 0.5% of total cells, $P < .01$) compared with the number of apoptotic cells in control cultures (4.0% ± 0.2% of total cells). Fenofibrate (100 μmol/L) significantly diminished apoptotic cell number, but this effect of fenofibrate was abolished in the presence of compound C or L-NAME (Fig. 6B).

In cells undergoing apoptosis, phosphatidyl serine is exposed at the outer leaflet of plasma membrane. Annexin V binds specifically to phosphatidyl serine, allowing the discrimination between viable and apoptotic cells [19,20]. Human glomerular microvascular endothelial cells were stained with annexin V and were detected by flow cytometry and quantified. High glucose significantly increased the

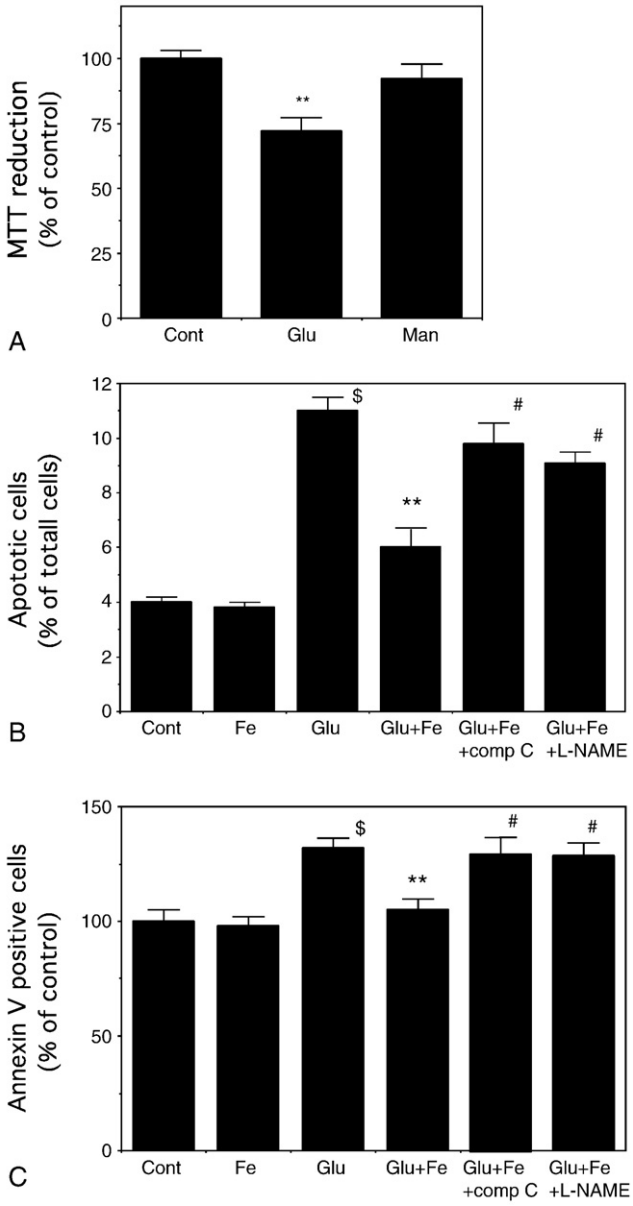

Fig. 6. A, High glucose decreases microvascular endothelial cell viability. Human glomerular microvascular endothelial cells were exposed to 5.5 mmol/L glucose (Cont), 30 mmol/L glucose (Glu), or 24.5 mmol/L mannitol (Man + 5.5 mmol/L glucose) for 6 days. The results are presented as percentage of control. B, High glucose increases apoptosis, and fenofibrate (Fe) diminished the apoptotic cell number. Human glomerular microvascular endothelial cells were exposed to 5.5 mmol/L glucose (Cont) or 30 mmol/L glucose (Glu) in the absence and presence of compound C (1 mmol/L) or L-NAME (100 μmol/L) for 6 days. The results are presented as percentage of total number of cells. C, Fenofibrate (Fe) inhibits high-glucose–induced early apoptosis. Human glomerular microvascular endothelial cells were exposed to 5.5 mmol/L glucose (Cont) or 30 mmol/L glucose (Glu) in the absence and presence of compound C (1 mmol/L) or L-NAME (100 μmol/L) for 6 days. The results are presented as percentage of annexin V–positive cells compared with control. Each bar represents the mean ± SEM (n = 4). $^{\$}P < .01$ compared with control; $^{**}P < .01$ compared with glucose; $^{\#}P < .05$ compared with high glucose + fenofibrate.

number of annexin V (+) cells (132.8% ± 6.2% of the control, $P < .01$). Fenofibrate (100 μmol/L) significantly diminished annexin V (+) cell number, but this effect of fenofibrate was reversed in the presence of compound C or L-NAME (Fig. 6C).

4. Discussion

In the present study, we demonstrate that fenofibrate activates AMPK by promoting AMPK phosphorylation. Adenosine monophosphate–activated protein kinase activation in turn activates eNOS through phosphorylation of Ser-1177, thereby increasing eNOS activity and producing more NO in HGMEC. Adenosine monophosphate–activated protein kinase directly phosphorylated Ser-1177 in association with eNOS activation; however, Akt phosphorylation occurred at the same rate as AMPK and eNOS phosphorylation in the present study, suggesting that Akt may also be involved in eNOS phosphorylation [21]. Although we did not perform a strict kinase assay for AMPK, we are certain that fenofibrate activates AMPK because the extent of AMPK phosphorylation at Thr-172 strongly reflects its activity [22] and because phosphorylation of the AMPK consensus substrate, ACC, at Ser-79 was also observed [23].

It is interesting that fenofibrate, but not bezafibrate, resulted in AMPK phosphorylation in HGMEC and that phosphorylation of AMPK was observed only in vascular endothelial cells and not in hepatocytes. Fenofibrate dose-dependently diminished AGE-induced NF-κB activity, whereas bezafibrate did not affect the NF-κB activity, suggesting that NF-κB inhibition is tied to AMPK activation. Indeed, blocking AMPK activation attenuated fenofibrate-induced inhibition of NF-κB activation as well as the NF-κB–dependent expression of cell adhesion molecules. The PPARα activator WY14643 produced limited activation of AMPK in endothelial cells and hepatic cells, whereas the PPARα inhibitor MK886 did not affect fenofibrate-induced AMPK activation in HGMEC, suggesting that fenofibrate activates AMPK independently of PPARα.

We further demonstrated that fenofibrate inhibits the expression of proinflammatory and adhesion molecule genes by blocking the phosphorylation and subsequent degradation of IκBα. These data suggest that fenofibrate might suppress AGE-induced NF-κB activation before IκB phosphorylation. We also demonstrated stimulation of IκBα phosphorylation by AGE through induction of IKK activity, and inhibition of IKK activity and AGE-induced IκBα phosphorylation by fenofibrate. Thus, fenofibrate-activated AMPK may suppress NF-κB activation by inhibiting IKK activity in microvascular endothelial cells. It has been reported that aminoimidazole-4-carboxamide-1-β-ribofuranoside attenuates LPS-induced activation of NF-κB via down-regulation of IKK α/β activity in glial cells [24]. A similar mechanism is observed in vascular endothelial cells

[25], suggesting that AMPK activation may inhibit AGE-induced NF-κB activation by suppressing IKK activity in HGMEC.

It has been reported that adiponectin prevents endothelial cell apoptosis through AMPK activation, although the detailed mechanism by which this occurs has not been described [26]. In the present study, fenofibrate-induced inhibition of HGMEC apoptosis was abrogated by AMPK inhibitor or NO synthase inhibitor. Thus, fenofibrate might inhibit apoptosis through AMPK activation and subsequent NO production. The production of reactive oxygen species in response to hyperglycemia results in sustained NF-κB activation with subsequent downstream activation of JNK and caspase 3, and a reduction in AKT survival signaling, all of which contribute to apoptosis [27]. Adenosine monophosphate–activated protein kinase activation and NO production in response to fenofibrate might interrupt this apoptotic signaling pathway. However, recent reports suggest that endothelial cell apoptosis might occur via a caspase-independent mechanism [28]. Therefore, further investigation is necessary to clarify the mechanism by which fenofibrate inhibits endothelial cell apoptosis.

In conclusion, we have demonstrated that fenofibrate activates AMPK in endothelial cells of the microvasculature, resulting in increased NO production and reduced inflammation, as well as inhibition of apoptosis. The ability of fenofibrate to activate AMPK is of particular interest because AMPK has been shown to mediate the beneficial and bioprotective effects of several drugs and adipocytokines [8-11]. The potential microvascular benefit of fenofibrate is suggested by an observed reduction in the need for laser treatment of retinopathy as well as a delay in the progression of nephropathy. There is also a significant reduction in the risk of minor amputations in the absence of large-vessel disease, as observed in the FIELD study [2-4]. Our findings suggest that fenofibrate-induced AMPK activation occurs independently of PPARα in microvascular endothelial cells and may confer microvascular benefits.

Acknowledgment

We are grateful to Dr Kazumi Akimoto and Ms Hiroko Satoh for technical assistance.

References

[1] Keech A, Simes RJ, Barter P, Best J, Scott R, Taskinen MR, et al. Effects of long-term fenofibrate therapy on cardiovascular events in 9795 people with type 2 diabetes mellitus (the FIELD study): randomised controlled trial. Lancet 2005;366:1849-61.

[2] Keech AC, Mitchell P, Summanen PA, O'Day J, Davis TM, Moffitt MS, et al. Effect of fenofibrate on the need for laser treatment for diabetic retinopathy (FIELD study): a randomised controlled trial. Lancet 2007;370:1687-97.

[3] Wierzbicki AS. Fibrates in the treatment of cardiovascular risk and atherogenic dyslipidaemia. Curr Opin Cardiol 2009;24:372-9.

[4] Rajamani K, Colman PG, Li LP, Best JD, Voysey M, D'Emden MC, et al. Effect of fenofibrate on amputation events in people with type 2 diabetes mellitus (FIELD study): a prespecified analysis of a randomised controlled trial. Lancet 2009;373:1780-8.

[5] Ido Y, Carling D, Ruderman N. Hyperglycemia-induced apoptosis in human umbilical vein endothelial cells: inhibition by the AMP-activated protein kinase activation. Diabetes 2002;51:159-67.

[6] Cacicedo JM, Yagihashi N, Keaney Jr JF, Ruderman NB, Ido Y. AMPK inhibits fatty acid-induced increases in NF-kappaB transactivation in cultured human umbilical vein endothelial cells. Biochem Biophys Res Commun 2004;324:1204-9.

[7] Murakami H, Murakami R, Kambe F, Cao X, Takahashi R, Asai T, et al. Fenofibrate activates AMPK and increases eNOS phosphorylation in HUVEC. Biochem Biophys Res Commun 2006;341:973-8.

[8] Zhou G, Myers R, Li Y, Chen Y, Shen X, Fenyk-Melody J, Wu M, et al. Role of AMP-activated protein kinase in mechanism of metformin action. J Clin Invest 2001;108:1167-74.

[9] Fryer LG, Parbu-Patel A, Carling D. The anti-diabetic drugs rosiglitazone and metformin stimulate AMP-activated protein kinase through distinct signaling pathways. J Biol Chem 2002;277:25226-32.

[10] Yamauchi T, Kamon J, Minokoshi Y, Ito Y, Waki H, Uchida S. Adiponectin stimulates glucose utilization and fatty-acid oxidation by activating AMP-activated protein kinase. Nature Medicine 2002;8:1288-95.

[11] Minokoshi Y, Kim YB, Peroni OD, Fryer LG, Muller C, Carling D, et al. Leptin stimulates fatty-acid oxidation by activating AMP-activated protein kinase. Nature 2002;415:339-43.

[12] Hattori Y, Suzuki M, Hattori S, Kasai K. Globular adiponectin upregulates nitric oxide production in vascular endothelial cells. Diabetologia 2003;46:1543-9.

[13] Bredt DS, Snyder SH. Nitric oxide mediates glutamate-linked enhancement of cGMP levels in the cerebellum. Proc Natl Acad Sci U S A 1989;86:9030-3.

[14] Heller R, Unbehaun A, Schellenberg B, Mayer B, Werner-Felmayer G, Werner ER. L-Ascorbic acid potentiates endothelial nitric oxide synthesis via a chemical stabilization of tetrahydrobiopterin. J Biol Chem 2001;276:40-7.

[15] Hattori Y, Suzuki M, Hattori S, Kasai K. Vascular smooth muscle cell activation by glycated albumin (Amadori adducts). Hypertension 2002;39:22-8.

[16] Kamata H, Manabe T, Oka S, Kamata K, Hirata H. Hydrogen peroxide activates IkappaB kinases through phosphorylation of serine residues in the activation loops. FEBS Lett 2002;519:231-7.

[17] Yamagishi S, Inagaki Y, Okamoto T, Amano S, Koga K, Takeuchi M, et al. Advanced glycation end product–induced apoptosis and overexpression of vascular endothelial growth factor and monocyte chemoattractant protein–1 in human-cultured mesangial cells. J Biol Chem 2002;277:20309-15.

[18] Mosmann T. Rapid colorimetric assay for cellular growth and survival: application to proliferation and cytotoxicity assays. J Immunol Methods 1983;65:55-63.

[19] Pepper C, Thomas A, Tucker H, Hoy T, Bentley P. Flow cytometric assessment of three different methods for the measurement of in vitro apoptosis. Leuk Res 1998;22:439-44.

[20] Vermes I, Haanen C, Reutelingsperger C. Flow cytometry of apoptotic cell death. J Immunol Methods 2000;243:167-90.

[21] Schulz E, Schuhmacher S, Münzel T. When metabolism rules perfusion: AMPK-mediated endothelial nitric oxide synthase activation. Circ Res 2009;104:422-4.

[22] Hardie DG. The AMP-activated protein kinase pathway—new players upstream and downstream. J Cell Sci 2004;117:5479-87.

[23] Dagher Z, Ruderman N, Tornheim K, Ido Y. Acute regulation of fatty acid oxidation and amp-activated protein kinase in human umbilical vein endothelial cells. Circ Res 2001;88:1276-82.

[24] Giri S, Nath N, Smith B, Viollet B, Singh AK, Singh I. 5-Aminoimidazole-4-carboxamide-1-beta-4-ribofuranoside inhibits

proinflammatory response in glial cells: a possible role of AMP-activated protein kinase. J Neurosci 2004;24:479-87.

[25] Hattori Y, Suzuki K, Hattori S, Kasai K. Metformin inhibits cytokine-induced NF-kB activation via AMPK activation in vascular endothelial cells. Hypertension 2006;47:1183-8.

[26] Kobayashi H, Ouchi N, Kihara S, Walsh K, Kumada M, Abe Y, et al. Selective suppression of endothelial cell apoptosis by the high molecular weight form of adiponectin. Circ Res 2004;94:e27-e31.

[27] Ho FM, Lin WW, Chen BC, Chao CM, Yang CR, Lin LY, et al. High glucose-induced apoptosis in human vascular endothelial cells is mediated through NF-kappaB and c-Jun NH2-terminal kinase pathway and prevented by PI3K/Akt/eNOS pathway. Cell Signal 2006;18:391-9.

[28] Leal EC, Aveleira CA, Castilho AF, Serra AM, Baptista FI, Hosoya K, et al. High glucose and oxidative/nitrosative stress conditions induce apoptosis in retinal endothelial cells by a caspase-independent pathway. Exp Eye Res 2009;88:983-91.